Testing Possible Scenario-Based Responses of Vegetation Under Expected Climatic Changes in Khuzestan Province

Authors: Eskandari Damaneh, Hadi, Jafari, Meysam, Eskandari Damaneh, Hamed, Behnia, Marjan, Khoorani, Asadollah, et al.

Source: Air, Soil and Water Research, 14(1)

Published By: SAGE Publishing

URL: https://doi.org/10.1177/11786221211013332

Testing Possible Scenario-Based Responses of Vegetation Under Expected Climatic Changes in Khuzestan Province

Air, Soil and Water Research
Volume 14: 1–17

DOI: 10.1177/11786221211013332

Hadi Eskandari Damaneh[1], Meysam Jafari[2], Hamed Eskandari Damaneh[2], Marjan Behnia[2], Asadollah Khoorani[1] and John P. Tiefenbacher[3]

[1]University of Hormozgan, Iran. [2]University of Tehran, Iran. [3]Texas State University, USA.

ABSTRACT: Projections of future scenarios are scarce in developing countries where human activities are increasing and impacting land uses. We present a research based on the assessment of the baseline trends of normalized difference vegetation index (NDVI), precipitation, and temperature data for the Khuzestan Province, Iran, from 1984 to 2015 compiled from ground-based and remotely sensed sources. To achieve this goal, the Sen's slope estimator, the Mann-Kendall test, and Pearson's correlation test were used. After that, future trends in precipitation and temperature were estimated using the Canadian Earth System Model (CanESM2) model and were then used to estimate the NDVI trend for two future periods: from 2016 to 2046 and from 2046 to 2075. Our results showed that during the baseline period, precipitation decreased at all stations: 33.3% displayed a significant trend and the others were insignificant ones. Over the same period, the temperature increased at 66.7% of stations while NDVI decreased at all stations. The NDVI–precipitation relationship was positive while NDVI–temperature showed an inverse trend. During the first of the possible future periods and under the RCP2.6, RCP4.5, and RCP8.5 scenarios, NDVI and precipitation decreased, and temperatures significantly increased. In addition, the same trends were observed during the second future period; most of these were statistically significant. We conclude that much assessments are valuable and integral components of effective ecosystem planning and decisions.

KEYWORDS: climate change, vegetation responses, NDVI, Mann-Kendall test, RCP scenarios, CanESM2 model

TYPE: Original Research

CORRESPONDING AUTHOR: Asadollah Khoorani, Department of Geographical Sciences, University of Hormozgan, Bandar Abbas, Hormozgan, P.O. Box 3995, Iran.
Email: khoorani@hormozgan.ac.ir

Introduction

In the mid-1980s, atmospheric temperatures were detectably and dramatically increasing in most parts of the world with projections indicating warming of 2.6 to 4.8 °C by the year 2100 (Intergovernmental Panel on Climate Change [IPCC] et al., 2013). Changing climates are now undeniably real and perceptible, and global warming is an immediate global challenge that can affect other spheres such as greenhouse emissions, soil quality, or land uses (Dore, 2005; Ghorbani et al., 2021; Shimizu et al., 2019). Due to the warming-induced change in average temperatures, precipitation variability and seasonality, unproductive nature of climate change is a key variable that can provide insights into the dynamics of the Earth's ecosystems over the 20th century; an era of industrialization, population growth, and greenhouse gas emissions that has generated serious global threats to the integrity and resilience of the Earth's ecosystems (Batllori et al., 2013). The increasing global temperature stems primarily from greenhouse gas emissions (Y. Yan et al., 2019). The global trend can be consequently interpreted and perceived by local factors and yields diverse shifts in components of regional climates, and thus the potential for significant departures from expected local conditions (Lee et al., 2015; Rebetez, 1996; Savari et al., 2021).

Due to these reasons, the arid and semi-arid regions and their sensitive and vulnerable ecosystems are heavily impacted by global warming, reducing species richness, degrading wildlife population structures, and changing the behaviors of and activities among species (Kharuk et al., 2007; Pereira et al., 2010; Rathore et al., 2019; Shagega et al., 2019). As an inevitable result of climate change, these regions have also been experiencing and will continue to undergo dramatic variations in the patterns of precipitation at least through the 21st century (Afreen & Singh, 2019). The Intergovernmental Panel on Climate Change's (IPCC) Fifth Assessment Report (AR5) provides an overview of the global-scale changes and potential future impacts of climate change, stating that the negative effects of these changes outweigh the positive ones. For instance, precipitation will tend to decrease in most parts of the world and it will be accompanied by significant adverse impacts on vegetation that may otherwise help to reduce greenhouse gas concentrations and help to return to and maintain stable climates (Cooper, 2019; Duffy et al., 2015; IPCC et al., 2013; T. Yan et al., 2019).

Climate is a key factor influencing the global distribution of vegetation (Burry et al., 2018; Chuai et al., 2013; Y. Zhang et al., 2013). Recent research shows that vegetation dynamics and variability are useful indicators of atmospheric anomalies and interactions (Ali et al., 2019; Hou et al., 2019). Hence, understanding how climatic factors affect vegetation requires an in-depth knowledge of the relationship between these factors and vegetation (Muradyan et al., 2019). In this case, remote sensing (RS)-based indices provide simple and cost-effective means for the spatiotemporal investigation of the connection between vegetation and its influencing factors (Chu et al., 2019; Eskandari et al., 2016). Vegetation is indirectly dependent upon

precipitation, temperature, drainage, mineralogical composition, soil type, and other factors that influence plant growth (Burry et al., 2018).

Foremost among the RS vegetation indices is the normalized difference vegetation index (NDVI), which accurately reflects the status and vigor of vegetation and its characteristics using reflective signatures (Hou et al., 2019; Lamchin et al., 2018). For example, in a study on the relationship between vegetation cover and climatic data, Hou et al. (2019) highlighted the value of NDVI for determining the effects of variations of precipitation and temperature as measures of climate and global warming on vegetation cover. Chu et al. (2019) studied the long-term response of vegetation to climate change and found a strong consistency between changes in seasonal vegetation from NDVI and climate change. These and many other studies in this field have acknowledged the capabilities of analyses of long-term NDVI to reflect changes in land surface characteristics and the responses of ecosystems to changes in climates.

It is worthy to highlight that unpredictable temperatures and precipitation variability are among the most severe consequences of climate change. They have been found repeatedly to be associated with the risks of floods and droughts and reduced agricultural productivity and plant diversity (Choo et al., 2019; Croke et al., 2017). Hence, it is both scientifically and practically imperative to deepen our understanding of the spatiotemporal variability of precipitation and temperature (Alimoradi et al., 2017; Tabari & Talaee, 2011; Tošić, 2004) and their potential future impacts on vegetation under different scenarios. Although much research has been directed toward the spatiotemporal variability of changing climates, the evidence is not yet clear about their future impacts. In general, studies in this field have predicted contradictory conditions regarding fluctuating temperature patterns and precipitation variability. Therefore, this study assesses past changes of temperature, precipitation, and NDVI during the period from 1984 to 2015 to project future changes and the impacts on vegetation dynamics for two future periods from 2014 to 2045 and 2045 to 2075. To achieve these goals, the Sen's slope estimator, the Mann-Kendall test, and Pearson's correlation test were used. After that, we hypothesize that future trends in precipitation and temperature could be accurately estimated using the Canadian Earth System Model (CanESM2) model and then used to estimate the NDVI trend for two future periods.

Material and Methods

This study was conducted in the Khuzestan Province, located in the south-western part of Iran, north of the westernmost part of the Persian Gulf. With an area of about 63,238 km^2, this province extends from 20° to 30°N and 47.7° to 50.5°E (Figure 1). Most of the province is covered by the Zagros Mountains forests, which are drained by two major rivers: the Karun and the Karkheh. These rivers form a broad alluvial fan in the southern portion of the province. Khuzestan's rivers account for approximately 30% of the country's surface waters (Moazami et al., 2014). The plains of this province, however, have a desert climate with very warm and dry summers. Precipitation in this province falls mostly during the winter and ranges from 300 mm in the plains to 500 mm toward highlands (Ghaemi et al., 2017).

Data used

Remote sensing data. NDVI was used to assess the trends of vegetation cover over time. NDVI is one of the most widely applied and useful RS-based vegetation indices (Gouveia et al., 2017; Tucker et al., 2005). It is highly sensitive to vegetation cover changes but less sensitive to the effects of the atmospheric and soils (except for areas with sparse vegetation). NDVI is calculated using equation (1)

$$NDVI = \frac{(NIR - R)}{(NIR + R)} \quad (1)$$

where *NIR* is the reflection of near-infrared wavelength and *R* is the reflection of visible red wavelength (Pinzon & Tucker, 2014). NDVI values range from −1 to +1. Higher values indicate denser vegetation covers (Higginbottom & Symeonakis, 2014). Most previous studies have used NDVI primarily for the analysis of vegetation growth (H. K. Zhang & Roy, 2016). Maps of NDVI derived from data gathered by NOAA's Advanced Very High-Resolution Radiometer (AVHRR) at a resolution of 8 km were obtained from the NASA Global Inventory Modelling and Mapping Studies (GIMMS) website (https://ecocast.arc.nasa.gov/data/pub/gimms). The NASA GIMMS AVHRR Global NDVI maps are geometrically and atmospherically calibrated and offer great opportunities for investigation of the effects of climate change on vegetation and for monitoring vegetation dynamics (Pinzon & Tucker, 2014). The maximum value composite (MVC) approach was applied to these maps to produce annual GIMMS NDVI maps (Gouveia et al., 2017; Zhao et al., 2018). Moreover, only pixels with mean annual NDVI > 0.1 were included in the vegetation analysis (Chu et al., 2019; Qi et al., 2019).

Climatic data. Future decadal changes in the province's temperature and precipitation were projected using the Statistical Downscaling Model (SDSM 4.2). This model provides an effective means for statistical downscaling of the general circulation model (GCM) outputs. SDSM 4.2 was developed by Wilby and Dawson (2013). The downscaling process with this model finds a meaningful relationship between the climatic variables recorded at ground stations (predictants) and large-scale atmospheric variables (predictors)

Large-scale atmospheric variables including the National Centers for Environmental Prediction (NCEP) predictors

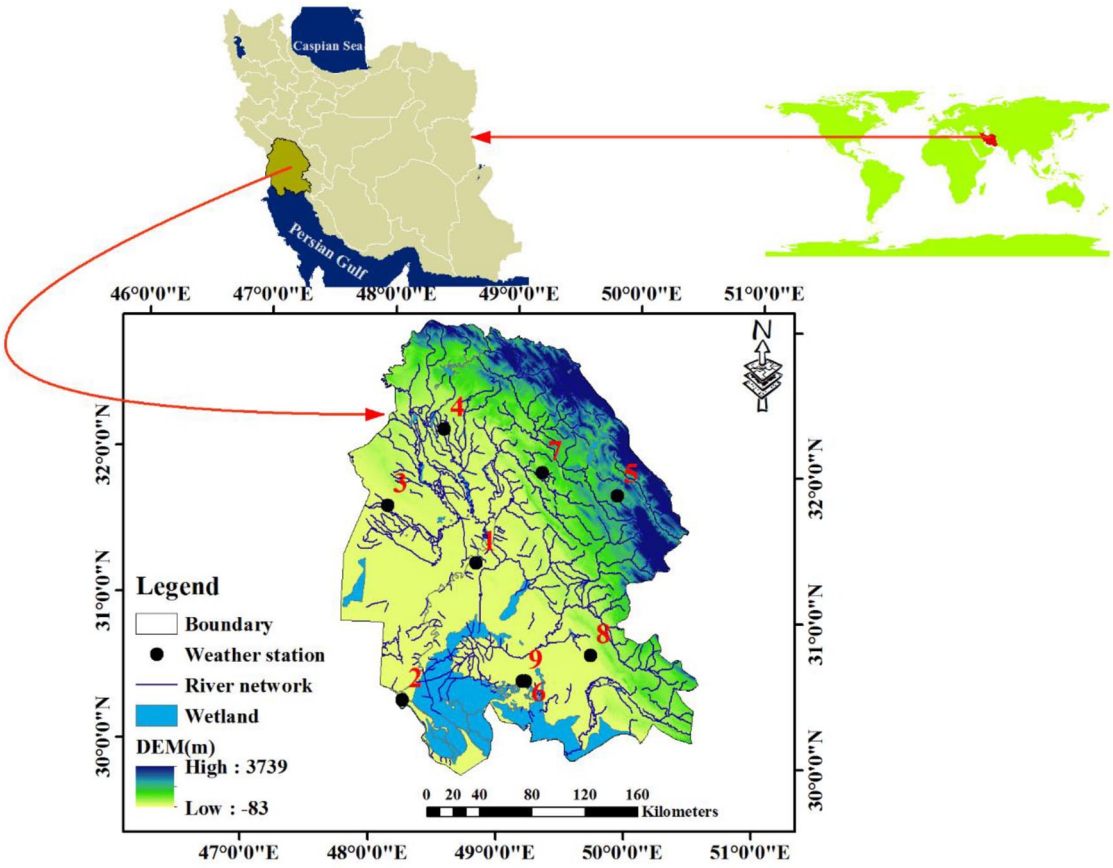

Figure 1. Location of the study area showing the topographical conditions, river network, synoptic stations, and wetlands of the Khuzestan province (bottom). 1 = Ahvaz station, 2 = Abadan station, 3 = Bostan station, 4 = Dezful station, 5 = Izeh station, 6 = Mahshahr station, 7 = Masjedsolyman station, 8 = Omidaghjari station, and 9 = Ramhormoz station

Table 1. Specifications of the CanESM2 General Circulation Model Available as the Input of SDSM4.2 Software.

CO_2 CONCENTRATIONS	RADIATIVE FORCING (W/M^2)	PROJECTION UNDER SCENARIO	RESOLUTION	MODEL
490 PPM before 2100 and then reduce	Its maximum value to 3 W/m^2 and then reduced	RCP2.6	2.8125° × 2.7906°	CanESM2
690 PPM remains stable after 2100	Its maximum value to 4.5 W/m^2 after 2100 remains stable	RCP4.5		
1370 PPM to 2100	More than 8.5 W/m^2 in 2100	RCP8.5		

CanESM2: Canadian Earth System Model; PPM: Parts per Million; RCP: representative concentration pathway.

for the period 1961–2005 that covers our baseline period and the outputs of the large-scale CanESM2 (Wu et al., 2017) under available scenarios for the baseline period and two future projection periods (2016–2045 and 2046–2075) were obtained from the Canadian Climate Data and Scenarios (CCDS) website (Table 1). The predictors of this model were normalized by the mean and standard deviation of the daily precipitation and temperature data of Khuzestan Province's synoptic stations, which were obtained from the Iranian Meteorological Organization for the years 1984 to 2005. Partial correlation analysis was conducted among the predictors and between the predictors and the predictants to identify and select the most suitable predictors with the strongest significant relationships with the observed precipitation and temperature at the significance level of 5%. The selected predictors were then used to build a multiple regression model for each month of the year for each station.

The performance of the CanESM2 model in predicting daily precipitation and temperature was evaluated by R^2 (equation [2]) and root mean square error (RMSE) (equation [3])

$$R^2 = \left\{ \frac{\sum_{i=1}^{T} \left(A_{obs,t} - \bar{A}_{obs}\right) \times \left(F_{model,t} - \bar{F}_{model}\right)}{\left[\sum_{i=1}^{T} \left(A_{obs,t} - \bar{A}_{obs}\right)^2\right]^{0.5} \times \left[\sum_{i=1}^{T} \left(F_{model,t} - \bar{F}_{model}\right)^2\right]^{0.5}} \right\}^2 \quad (2)$$

$$\text{RMSE} = \sqrt[2]{\frac{1}{n}\sum_{i}^{n}\left(A_t - F_t\right)^2} \quad (3)$$

where it is the observed value, F_t is the predicted value and n is the number of data. Therefore, the appropriate range of evaluation coefficient R^2 is presented in Table 2. Also Figure 2 shows the steps undertaken for climate downscaling.

Finally, according to the statistical equations and the regression model fitted between large-scale NCEP predictors and observed precipitation and temperature, the downscaling process was performed on the CanESM2 model outputs under RCP2.6, RCP4.5, and RCP8.5 scenarios. Finally, station-scale daily precipitation and temperature data were simulated for the two future periods (Figure 2).

Table 2. The Coefficient of the Model's Assessment and the Range of Coefficient Identification (Moriasi et al., 2007).[43]

CLASS	COEFFICIENT OF DETERMINATION (R^2)
Very good	$.866 \leq R^2 < 1$
Good	$.733 \leq R^2 < .866$
Satisfactory	$.6 \leq R^2 < .733$
Unsatisfactory	$R^2 < .6$

Trends of vegetation cover and climatic variables. The Mann-Kendall Test statistic, S, is estimated by equation (4) and the significance of the trend is determined by calculating the z-statistic (equation [5])

$$S = \frac{\sum_{i=1}^{n}\sum_{j=i+1}^{n} sgn\left(Y_j - Y_i\right)}{\sigma_s} \quad (4)$$

$$z = \begin{cases} \dfrac{s-1}{\sqrt{var\left(s\right)}} \; when \; s > 0 \\ 0 \; when \; s = 0 \\ \dfrac{s-1}{\sqrt{var\left(s\right)}} \; when \; s < 0 \end{cases} \quad (5)$$

in which σ_s is the standard deviation of the data, n is the number of data, Y_j and Y_i are the data values for consecutive periods, $sgn(Y_j - Y_i)$ is 1, 0, or −1, implying an ascending trend, the lack of a trend, and a descending trend, respectively. Also, var(s) is a variance of the S-statistic (Zheng et al., 2018). The trend is significant at the 5% level if $|z| \geq 1.96$ (Sen, 1968). The trend magnitude is also estimated by using the age estimator slope (Tabari & Talaee, 2011). In other words, the time series is considered a linear trend with noise, and the estimator (Theil-Sen [β]) can be used to determine a change in the slope of the hydrological time series, vegetation cover time series, and methodological time series xi (I = 1, 2, . . ., n) (Tabari & Talaee, 2011) (equation [6])

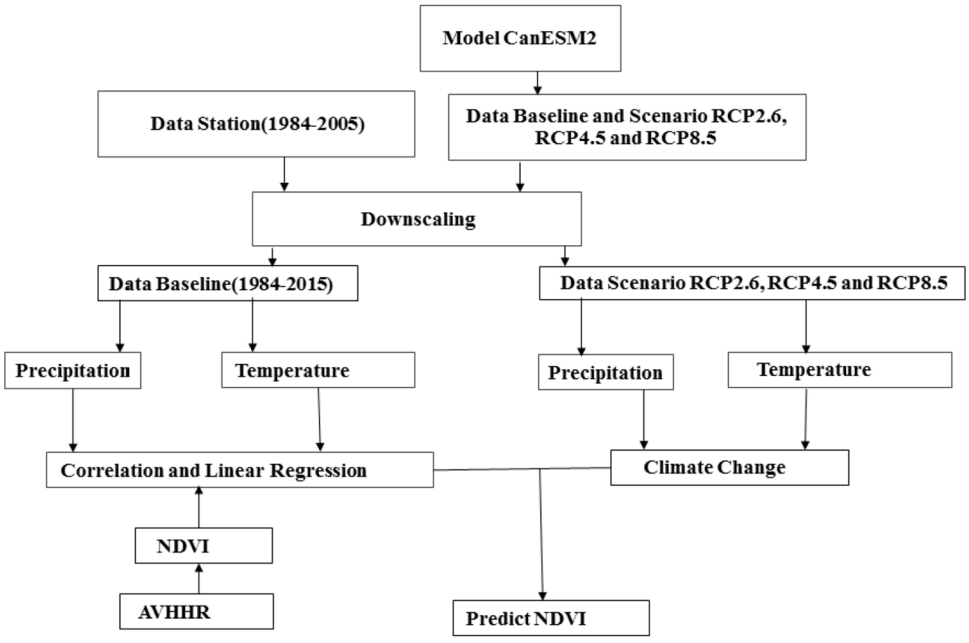

Figure 2. Steps performed for precipitation and temperature downscaling using SDSM4.2.

$$\beta = Median\left[\frac{Xj - Xi}{j - i}\right] \forall 1 < i < j < n \quad (6)$$

in which X_i and X_j represent data points at times i and j, respectively, and β represents the slope of the trend line whose positive (negative) values imply an ascending (descending) trend of the time series.

Linear regression between climatic parameters and vegetation cover. After fitting the CanESM2 model's outputs, the relationship between NDVI and precipitation and temperature predictions was determined by regression analysis. The model is shown in equation (7)

$$NDVI = b + b \times P + b \times T \quad (7)$$

Where P is monthly precipitation, T is monthly temperature and b, b1, and b2 are undermined coefficients determined by the least square method. After analyzing the trends of climatic data and NDVI, the association between these variables was investigated using correlation analysis in which NDVI was the dependent variable and precipitation and temperature were the independent variables.

Climatic parameters are the most important factors influencing vegetation cover conditions. The assessment of the quantitative relationship between vegetation cover pattern and climatic parameters is one of the main applications of remote sensing on a global and regional scale. Precipitation and temperature directly affect water balance and they are, in turn, two of the factors that are responsible for the variation in soil moisture and plant growth. The extended DeMartonne method from Rahimi et al. (2013) and Ahmadaali et al. (2021) was used for climate classification. According to mentioned classification, the climate of stations 1, 3, 4, 6, 8, and 9 were Arid; and also the climate of stations 2, 5, and 7 were Hyper-Arid, Mediterranean and Semi-Arid, respectively.

Predicting vegetation changes using climatic scenarios. Based on the relationships between precipitation and temperature and NDVI at each station, changes in the province's vegetation were simulated under three scenarios from the fifth climate change report including RCP2.6, RCP4.5, and RCP8.5 for the periods 2016 to 2045 and 2046 to 2075 (Ortiz-Jiménez, 2018).

Results

Performance evaluation of CanESM2 climate model

The performance of the CanESM2 model was validated by comparing the model predictions made for the years 1984–2005 with data observed on the ground during this period. Table 3 shows the R^2 and RMSE values computed between simulated and observed data. According to RMSE values, the least simulation error achieved for precipitation (6.60 mm) and temperature (1.50°C) occurred for data from the Mahshahr Station. These

Table 3. Performance of the CanESM2 Model.

STATISTICAL	PARAMETER	AHVAZ	ABADAN	BOSTAN	DEZFUL	IZEH	MAHSHAHR	MASJEDSOLYMAN	OMIDAGHJARI	RAMHORMOZ
RMSE	Precipitation	13.85	8.39	6.71	7.65	11.34	6.60	12.30	9.04	11.26
	Temperature	1.55	2.24	1.87	1.79	1.72	1.50	2.09	1.99	2.07
R^2	Precipitation	.77	.83	.95	.97	.98	.96	.96	.93	.96
	Temperature	.99	.99	.99	.99	.99	.99	.99	.99	.99

CanESM2: Canadian Earth System Model; RMSE: root mean square error.
Significant at $p < .05$.

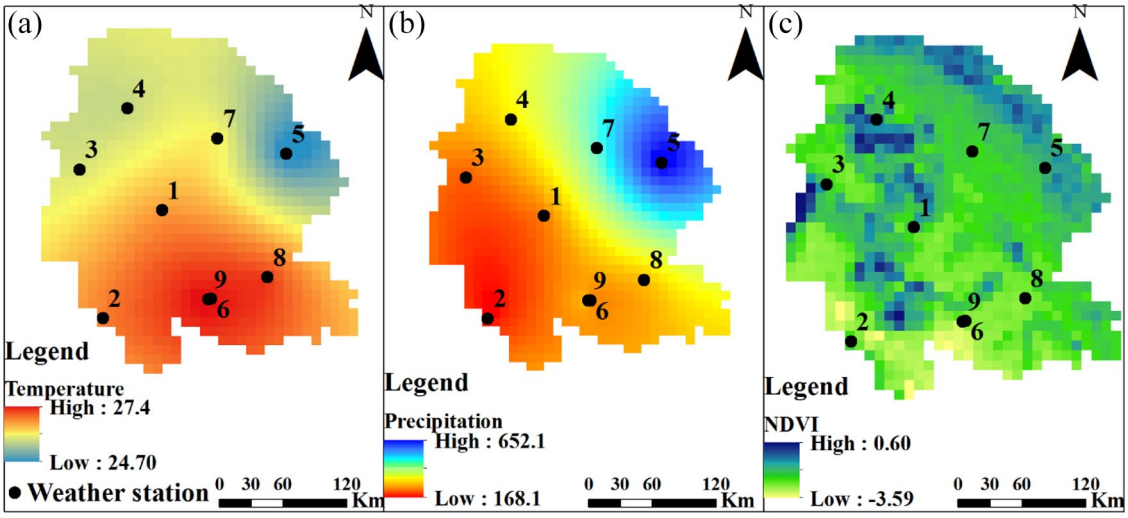

Figure 3. Mean spatial distribution of (a) temperature, (b) precipitation, and (c) NDVI for the period 1984–2015.

findings are consistent with Pullens et al. (2019) which assessed the effects of climate change on European winter oilseed rape. According to their results, the best performing model was built for Czechia while the poorest performing was for Germany with RMSE values of 20.6 and 19.2, respectively. The predicted temperature of the CanESM2 model was determined by statistical indices as very good in all synoptic stations of Khuzestan Province based on several studies (Choi et al., 2019; El-Samra et al., 2018; Moriasi et al., 2007; Worku et al., 2018). In terms of precipitation predictions, all stations fell into a very good class, except for Ahvaz and Abadan stations, which were classified as good.

Spatial distribution of precipitation, temperature, and NDVI in baseline (1984–2015)

The spatial distribution of the 31-year means temperature, NDVI, and precipitation values are shown in Figure 3(a) to (c), respectively. Interpolation of the temperature and precipitation data was performed using the inverse distance weighted (IDW) method. The temperature was found to be the highest in the south and lowest in the east and northeast of the province. The highest NDVI values were observed in the east, northeast, and adjacent to major rivers while the lowest values were concentrated in the south. The highest and lowest precipitation amounts were observed in the east-northeast and the south-southwest of the province, respectively. However, as other authors recently demonstrated, the elevated variability of the different weather types in arid and semi-arid areas make these irregularities relevant to be considered when we interpret these results (Peña-Angulo et al., 2019; Rodrigo-Comino et al., 2019).

Results of NDVI, temperature, and precipitation trend analysis for the period 1984–2015

Izeh Station received the highest amount of precipitation in the province (Table 4). This station, however, experienced the sharpest decline in precipitation (with a Z value of –2.73) over the past couple of decades. Masjed Soleiman Station was the second station experiencing a sharp precipitation decline. In general, precipitation in Khuzestan Province declined over the baseline period. Temperature decreased at Dezful, Masjed Soleiman, and Omidieh Aghajari stations. The highest temperature decline was observed in Omidieh Aghajari station with a Z value of –2.88. This trend at the other stations was in line with the global trend of warming as it was demonstrated by other authors applying predictive models (Braganza et al., 2004; Hansen et al., 2006, 2013; Pate, 2011).

In general, Khuzestan has experienced increasing temperature during the past decades. The sharpest decrease in NDVI was observed at Bostan Station at the significance level of 5% with a Z value of –4.11 while the largest increase was observed in Ramhormoz and Mahshahr stations with a Z value of 2.50. Except for Ramhormoz and Mahshahr stations, the vegetative cover is likely to be affected by precipitation because these parameters changed similarly across the province.

Regression relationship between vegetation cover, temperature, and precipitation

The correlation between NDVI and precipitation was negative at Ahvaz, Mahshahr, and Ramhormoz and positive at Abadan, Bostan, Dezful, Izeh, Masjed Soleiman, and Omidieh Aghajari. Of these, the statistical relationship between NDVI and precipitation at Omidieh Aghajari was the only that was significant. The NDVI–temperature relationship was negative at Ahvaz, Abadan, Bostan, Izeh Abadan, and Omidieh Aghajari, and of these, a significant relationship was observed only at Abadan (Figure 4). The NDVI–temperature relationship was positive, but statistically insignificant, at Mahshahr and Masjed Soleiman. It was negative in other stations (Table 5).

Table 4. Trend of Temperature, Precipitation, and NDVI at the Stations of Khuzestan Province.

STATION	PARAMETER	Z	SIG.
Ahvaz	Precipitation	–1.92	ns
	Temperature	4.31	***
	NDVI	–2.27	***
Abadan	Precipitation	–1.02	ns
	Temperature	1.12	ns
	NDVI	–2.89	***
Bostan	Precipitation	–0.37	ns
	Temperature	1.49	ns
	NDVI	–4.11	***
Dezful	Precipitation	–0.68	ns
	Temperature	–1.15	ns
	NDVI	–2.92	***
Izeh	Precipitation	–2.73	***
	Temperature	5.36	***
	NDVI	–1.15	ns
Mahshahr	Precipitation	–1.86	ns
	Temperature	0.93	ns
	NDVI	2.50	***
Majsedsolyman	Precipitation	–2.26	***
	Temperature	–0.03	ns
	NDVI	–0.67	ns
Omidaghjari	Precipitation	–0.34	ns
	Temperature	–2.88	***
	NDVI	–0.41	ns
Ramhormoz	Precipitation	–2.20	***
	Temperature	4.15	***
	NDVI	2.50	***

NDVI: normalized difference vegetation index; ns: NO TREND.
***TREND.

Future trends of NDVI and climatic variables relative to the baseline period

Under the RCP2.6 scenario, vegetation cover at Ramhormoz, Masjed Soleiman, Mahshahr, and Dezful stations will increase, compared with the baseline period, during the first future period, and during the second period (Table 6, Figure 5). Compared with the baseline period, precipitation at Ahvaz Station is projected to increase by 32.6% and 38.9% during the first and second future periods, respectively. The temperature at most stations would be expected to increase by 4%, but the increases at Abadan Station would be by 1.2% (first period) and 2.1% (second period).

Under the RCP4.5 scenario, vegetation coverage is projected to increase by at least 4% at the Ramhormoz, Masjed Soleiman, Mahshahr, and Dezful stations. In fact, the increase at the Mahshahr station in the first and second periods would be 26.1% and 42.3%, respectively. At other stations, vegetation would be expected to decrease during both periods. The Izeh station in the first and second periods will decrease by 8.4% and 13.9%. The temperature increases among all stations would be lowest in the first and second periods at the Aban (0.9% and 3.9%) and Bostan (4.3% and 7.4%). Precipitation was projected to increase more rapidly during the first period than the second period. It was also projected to decrease to a greater degree during the second period than during the first period. In the first period, the highest increase would occur at Ahvaz and Abadan (40.4% and 17.6%), while in the second period, the highest decrease would occur at Mahshahr and Izeh (27% and 23.9%).

Under the RCP8.5 scenario, vegetation cover would decline at Izeh and Ahvaz during the first period and at Ahvaz, Abadan, Bostan, and Izeh during the second period. In the first period, the largest decreases would occur at Izeh and Ahvaz (–9.5% and –8.3%) and at Izeh and Abadan (–20.1% and –19.7%) during the second period. The greatest increases of vegetation in both periods would occur at Mahshahr and Ramhormoz. Temperatures would increase at all stations. The lowest increases during both periods would occur at Abadan (1.5% in the first period and 8.7% in second) and Bostan (4.3% and 11.7%). During both periods, precipitation would decrease at most stations; the greatest in the first period would be at Mahshahr (–24.3%) and at Izeh (–37.9%) during the second period.

During the first future period under the RCP2.6, RCP4.5, and RCP8.5 scenarios, Izeh showed the largest expected temperature increases (2.10°C, 1.97°C, and 2.19°C). The smallest increases would occur at Abadan (0.4°C, 0.33°C, and 0.48°C) (Figure 6). During the second period, the greatest temperature increases would occur at Izeh (2.39°C, 3.02°C, and 4.20°C) and smallest increases (.063°C, 1.20°C, and 2.34°C) would occur at Abadan. Average temperatures across Khuzestan Province were projected to increase under the three scenarios by 1.41°C, 1.30°C, and 1.47°C in the first period and by 1.66°C, 2.26°C, and 3.41°C in the second period. Thus, the results show projections of increasing temperatures under the three scenarios.

Precipitation increased by 22.6%, 28.5% and 29.8% in the first period and by 40.7%, 35.3%, and 72.5% in the second period under the three scenarios. Precipitation was projected to increase at Abadan by 17.9% during the first period in scenario RCP2.6, and by 6.4% and 11.7% during the first period and 7.9% and 28.8% during the second period under scenarios RCP4.5 and RCP8.5. It would increase at Omidieh Aghajari by 2.9% and 0.9% in the first and second periods in scenario

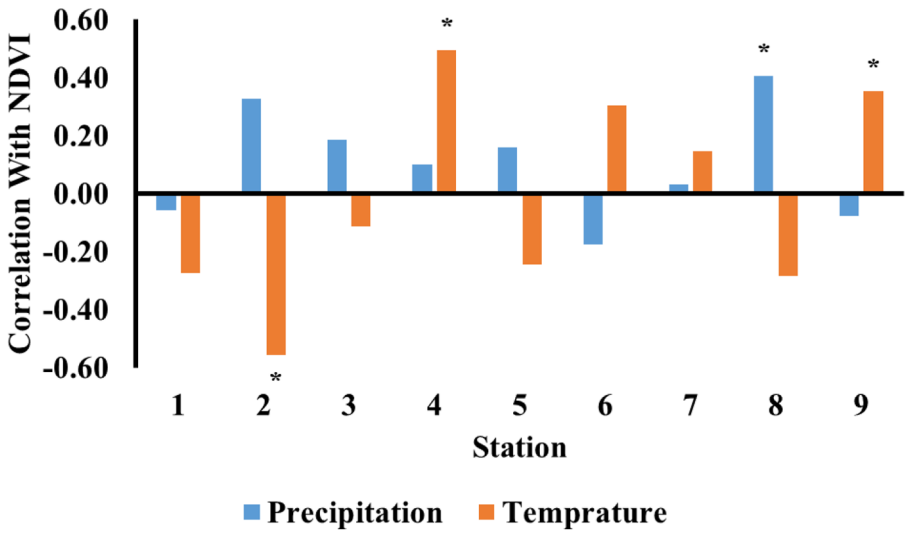

Figure 4. Correlation between NDVI, precipitation, and temperature during 1984–2015.
*Statistically significant relationship.

Table 5. Summary and Regression Formula for the Normalized Vegetation Index Using Mean Annual Precipitation and Temperature for Each Station and for the Entire Study Set.

STATION	EQUATION	*P* VALUE	R^2	RMSE
Ahvaz	0.344 – 0.000033 × P – 0.00704 × T	<.05	.1	0.01
Abadan	0.513 + 0.000042 × P – 0.01421 × T	<.05	.3	0.01
Bostan	0.361 + 0.000175 × P – 0.0063 × T	<.05	.03	0.08
Dezful	–0.494 + 0.000064 × P + 0.03157 × T	<.05	.2	0.04
Izeh	0.356 + 0.000009 × P – 0.00827 × T	<.05	.06	0.03
Mahshahr	–0.1039 – 0.000019 × P + 0.00545 × T	<.05	.1	0.01
Majsedsolyman	0.017 + 0.000014 × P + 0.00468 × T	<.05	.02	0.02
Omidaghjari	0.1530 + 0.000052 × P – 0.00318 × T	<.05	.2	0.01
Ramhormoz	–0.0812 + 0.000007 × P + 0.00411 × T	<.05	.36	0.01
Total equation	0.119 + 0.000071 × P + 0.00018 × T	<.05	.09	0.01

RMSE: root mean square error.

RCP2.6, and by 2.4% during the second period under scenario RCP4.5. With the exception of these two sites, precipitation would be expected to decrease at the other sites under all three scenarios and periods.

Vegetation is expected to increase at Dezful by 0.03, 0.03, and 0.02 during the first periods under the three scenarios, and by 0.05, 0.03, and 0.08 during the second periods. It would also increase at Mahshahr, at Masjed Soleiman, and at Ramhormoz. Vegetation cover was projected to decrease at the other five stations.

Climate change-based changes in NDVI

From 2016 to 2045, an increasing trend was projected for temperatures at all stations and under all scenarios, except for Abadan, Bostan, Mahshahr, and Masjed Soleiman under the RCP2.6 scenario where there seemed to be no trends (Figure 7). Precipitation was trending negatively at Mahshahr and Ramhormoz under the RCP8.5 scenario and at Dezful under the RCP4.5 scenario. The temperatures for the period from 2046 to 2075 were unchanging at Ahvaz, Bostan, Dezful, Izeh, Mahshahr, Masjed Soleiman, Omidieh Aghajari, and Ramhormoz under the RCP2.6 scenario and decreasing at Abadan under the RCP2.6 scenario. On the other hand, Sen's slope estimator indicated a positive increase at these stations in the future. Precipitation is projected to decrease significantly at Dezful and Izeh under the three scenarios. The trend of NDVI for the first period (Figure 7) decreased at Dezful and increased at Izeh with Z values of 2.02 and 2.073, respectively. During

Table 6. Percentage Change in NDVI and Climatic Variables Compared to the Baseline Period.

INDEX	STATION	PERIOD	2016–2045			2046–2075		
			SCENARIO			SCENARIO		
			2.6	4.5	8.5	2.6	4.5	8.5
Precipitation	Ahvaz	1984–2015	32.6	40.4	46.4	38.9	52.1	86.5
	Abadan		4.5	17.6	21.4	30.3	23.4	42.2
	Bostan		–9.6	–3.9	–7.7	–10.3	–17.8	–20.3
	Dezful		–10.1	–14.5	–13.9	–14.2	–22.8	–33.6
	Izeh		–12.8	–10.5	–13.8	–18.7	–23.9	–37.90
	Mahshahr		–15.0	–16.8	–24.3	–24.9	–27.0	–34.9
	Masjedsolyman		5.4	5.6	6.5	3.2	0.7	–6.5
	Omidaghjari		9.0	4.3	5.5	6.9	8.5	11.1
	Ramhormoz		–13.6	–11.7	–12.8	–19.7	–15.8	–30.3
Temperature	Ahvaz	1984–2015	5.0	4.7	5.3	5.8	8.3	12.8
	Abadan		1.2	0.9	1.5	2.1	4.3	8.6
	Bostan		4.2	3.9	4.3	4.9	7.4	11.6
	Dezful		6.0	5.5	6.1	7.2	9.6	14.2
	Izeh		7.6	7.1	8.0	8.9	11.6	16.7
	Mahshahr		5.9	5.9	6.7	7.1	9.5	13.7
	Masjedsolyman		5.7	4.7	5.5	6.4	8.7	13.3
	Omidaghjari		5.5	5.0	5.5	6.3	8.4	12.6
	Ramhormoz		4.9	4.5	5.2	6.1	8.3	12.9
NDVI	Ahvaz	1984–2015	–7.4	–7.4	–8.3	–8.7	–12.2	–19.2
	Abadan		–2.9	–1.6	–2.9	–3.9	–9.7	–19.7
	Bostan		–3.6	–2.6	–3.4	–4.2	–6.9	–10.1
	Dezful		14.7	13.1	14.7	17.4	23.0	34.2
	Izehr		–9.1	–8.4	–9.5	–10.7	–13.9	–20.1
	Mahshahr		25.1	26.1	30.4	24.0	42.3	61
	Masjedsolyman		4.8	4.1	4.8	5.4	7.2	10.7
	Omidaghjari		–4.1	–4.4	–4.8	–5.4	–7.3	–11.2
	Ramhormoz		15.8	14.7	16.9	19.5	27.2	41.7

NDVI: normalized difference vegetation index.

this period and under the other scenarios, the NDVI trend was insignificant: 33.3% of cases displayed positive trends and 44.4% negative. During the second period, NDVI also exhibited no trend under RCP2.6 with a positive change in 55.56% of cases and negative in 44.4%. Under the RCP4.5 scenario, the NDVIs during the first period were significant for all stations, 44.4% will experience positive change (the highest Z value of 4.59 observed at Mahshahr), and 55.6% will experience negative change (the lowest Z value of –4.26 was observed at Abadan). During the second period, NDVI was projected to increase at Mahshahr, Masjed Soleiman, and Ramhormoz but decrease at Omidieh Aghajari and Izeh. Under the RCP8.5 scenario, the vegetation trends were significant for both future periods. Vegetation was projected to increase at these locations by 44.4% and 33.3% of cases during the first period and decrease at 55.6% and 66.7% of cases during the second period.

The highest correlation coefficients between NDVI and temperature were at Abadan, Dezful, and Ramhormoz, and between

NDVI and precipitation at Ramhormoz (Table 7). These regression equations were used to simulate climate change–induced fluxes in NDVI for both future periods. The correlation between these two variables was highest under the RCP8.5 scenarios, followed by the RCP2.6 and RCP4.5 scenarios.

Discussion

Trend of climate variable NDVI during the baseline period

During the baseline period from 1984 to 2016, precipitation decreased at all meteorological stations in the province; 33.3% of these recorded statistically significant trends, while the other 66.77% of stations revealed no trends, which is consistent with Some'e et al. (2012) which reported that more than 30% of stations in Iran experienced decreasing precipitation during this period. Masoudi and Elhaeesahar (2016) examined precipitation and temperature in Khuzestan Province and found that precipitation increased at 7% of stations, decreased at 67.2%, and remained constant at 25.8%. Moreover, 88.3% of the province experienced increasing temperatures (T. Yan et al., 2019). NDVI increased by 77.7%. Although 57.1% of the area experienced increases that were statistically significant, 42.85% displayed no trends. The trends of vegetation were positively

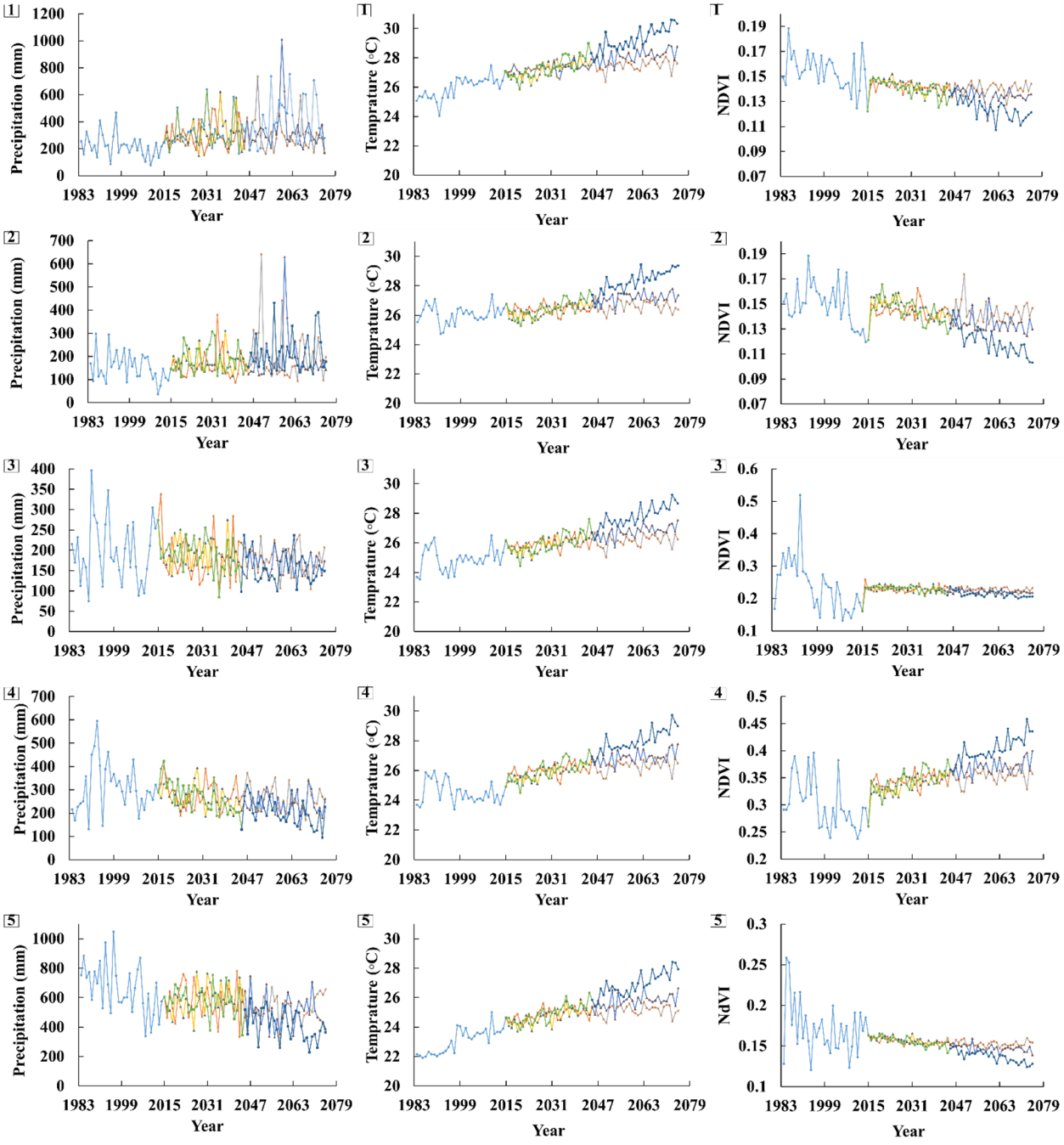

Figure 5. *(Continued)*

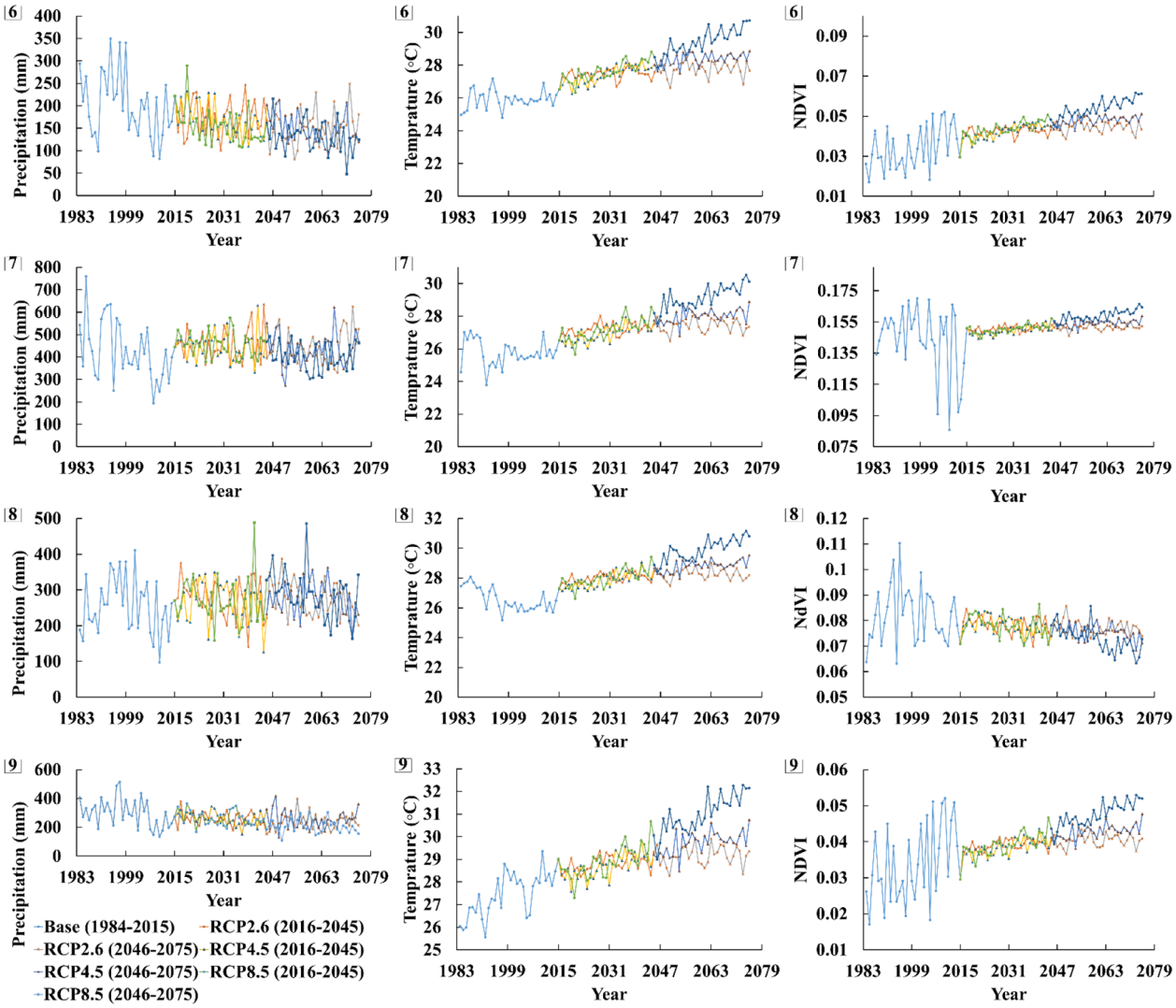

Figure 5. Trends of precipitation, temperature, and NDVI at Khuzestan synoptic stations under RCP2.6, RCP4.5, and RCP8.5 scenarios for two future periods: 2016–2045 and 2046–2075.

correlated to precipitation trends and negatively related to temperature trends, which is consistent with WenBin et al. (2011) and negatively related to temperature trends, which is in agreement with T. Yan et al. (2019) which reported that solar radiation and precipitation had significant impacts on vegetation, and also with Alimoradi et al. (2017). They highlighted that Land Surface Temperature (LST) determined more changes of NDVI than precipitation and air temperature. Also, Rathore et al. (2019) indicated that temperature and precipitation govern the distribution of *Taxus wallichiana*. Even, Hadian et al. (2019) indicate that high correlations between NDVI and climatic parameters signify a strong influence of climatic anomalies on vegetation and that drought-induced decreases in precipitation are tied to vegetation decline. The relationships between NDVI and precipitation and temperatures were found to not achieve statistical significance, which might be attributed to the arid and semi-arid climates that dominate Khuzestan Province (Gouveia et al., 2017; Wingate et al., 2019).

Performance of the CanESM2 model

The predictive performance of the CanESM2 model was evaluated using R^2 and RMSE. The model performance for temperature showed a good (R^2) and very good (RMSE) agreement because annual temperatures were more consistent than annual precipitation totals. However, the model produced a moderate and good performance for precipitation predictions. These results are in line with Khosravi et al. (2017) where the model's predictive performance (according to R^2 and RMSE) was higher for temperature. All nine stations were predicted to experience increasing temperatures during the two future periods relative to the baseline. Comparisons of increasing temperatures between the first and second period indicated that temperatures increased by 0.25°C, 0.96°C, and 1.94°C under the three scenarios. Therefore, it could be concluded that temperatures increase by 1.96°C from the RCP2.6 scenario to the RCP8.5 scenario. Other authors like Shagega et al. (2019) predicted future climates in the Ngerengere River

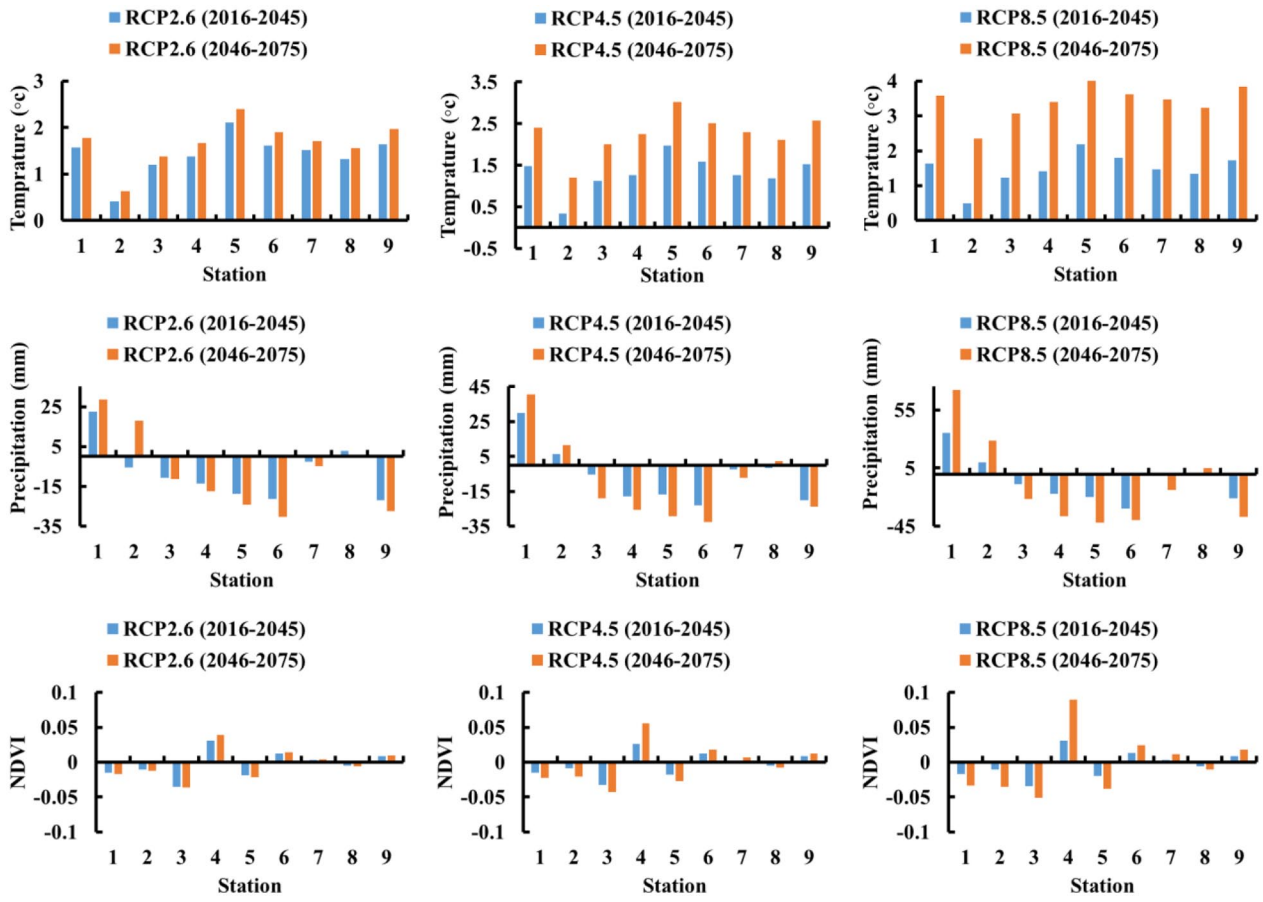

Figure 6. Percentage of change in vegetation, temperature and vegetation during the two future periods with respect to the baseline period.

watershed, Tanzania using Lars-WG and similarly found minimum and maximum temperature increases of 0.2°C and 2.6°C, respectively, during the 2050s and 2.7°C and 4.4°C during the 2080s. The temperature increases were maximal in October and November while minimal in June and July. Moreover, the precipitation trends were projected to reflect decreases of 12% to 37% in April, May, June, and July, and 3% to 58% increases in other months of the year. Another example can be found in Gaitán et al. (2019) in which predicted temperatures and cold and warm waves in Spain using the outputs of Coupled Model Intercomparison Project Phase 5 (CMIP5) and two downscaling steps. They found that climate change scenarios indicate there will be a gradual increase in maximum daily temperatures during the 21st century, with the greatest increase (7°C) during summers under the RCP8.5 scenario.

Projections and relationship of climate change and NDVI in future

Projections indicate increases in minimum temperatures as well, but at lower rates than the speed of warming of maximum temperatures. Minimums increased by only 3 and 5.6°C under the RCP4.5 and RCP8.5 scenarios by the end of the century. Our results are consistent with the findings of D'Oria et al. (2017), which reports that the climate of Tuscany, Italy, which predicted increasing temperatures during two future periods (2031–2040 and 2051–2060) of 0.8°C and 1.1°C under the RCP4.5 scenario and 0.9°C and 1.9°C under the RCP8.5 scenario. Irving et al. (2012) revealed that mean annual temperature in Australia is slated to increase by 3.2°C and 4.2°C under the RCP8.5 and RCP4.5 scenarios, respectively, during the period 2080–2099, relative to 1980–1999. In this study, precipitation was projected to increase at Ahvaz Station under all three scenarios, at Abadan Station in both future periods, and under all scenarios, except for the product of the RCP2.6 scenario during the first period, as well as at Omidieh Aghajari Station during the first future period under the RCP2.6 and for all stations under all future climate scenarios. These results indicate that the area can be expected to be wetter in the future. T. Yan et al. (2019) also found increasing trends of precipitation of 61% and 5.4% for both futures (2021–2035 and 2051–2065) given the RCP4.5 scenario, and 12.7% and 12.7% for both future periods under the RCP8.5 conditions. T. Yan et al. (2019) also projected precipitation increases in the Hindu Kush region of the Himalaya of 24% under the RCP8.5 scenario. This could be attributed to increasing atmospheric vapor pressure and global warming–induced changes in the water cycle of the atmosphere (D. F. Zhang et al., 2017). Our results showed a decreasing trend in precipitation at Bostan, Dezful, Izeh, Mahshahr, and Masjed

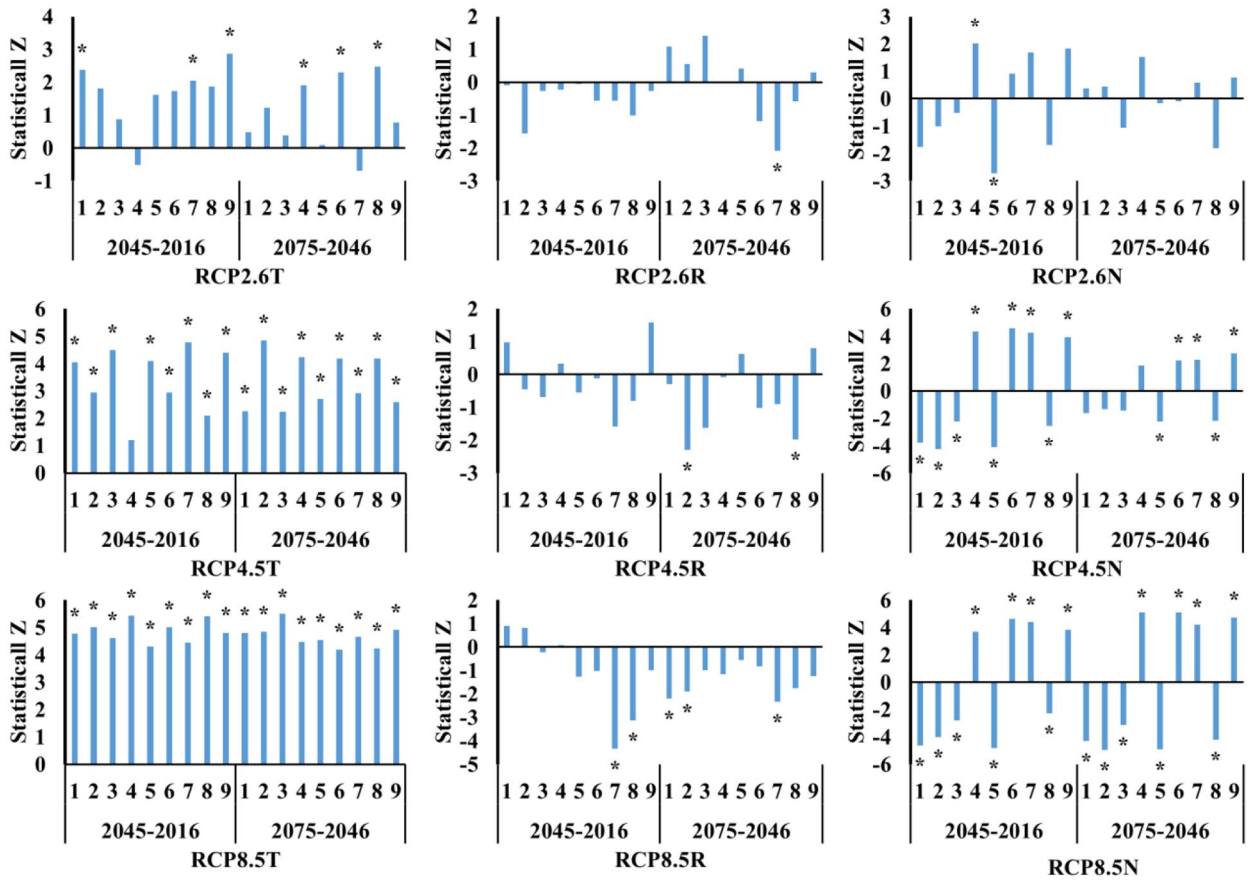

Figure 7. Trends of temperature (T), precipitation (R) and NDVI (N) during the two future periods.
*Significant relationship ($p < .05$).

Soleiman stations under all three scenarios. Precipitation at Mahshahr Station would decrease during the first future period and the second under the RCP2.6, RCP4.5, and RCP8.5 scenarios which are consistent with Gaitán et al. (2019) which indicates that precipitation in the upper reaches of the Jordan River is expected to decrease by 3.5% and 10.5% during the period from 2020 to 2049, and by 11% and 15.5% during the period from 2050–2079 under RCP4.5 and RCP8.5 conditions. Due to the specific patterns of precipitation in arid and semi-arid regions, the trends differed between stations. Projections of increasing temperature match the results of IPCC et al. (2013) and Gorguner et al. (2019), which suggest that mean annual temperature will increase under all scenarios during the 21st century. The increasing temperature projected under the RCP4.5 and RCP8.5 scenarios are in line with the predictions of the IPCC Fifth Assessment Report (IPCC). Precipitation projections showed a positive and negative statistically significant trend at some stations and, not significant trends in other stations, a finding that is consistent with Ishida et al. (2017), which showed no trend in precipitation in six sub-basins of the northern California watershed under the RCP4.5 and RCP8.5 scenarios and also related this precipitation sensitivity to climate change scenarios and with the results of Awal et al. (2016) and Keggenhoff et al. (2014). Precipitation exhibited no clear trends and only indicated a few abrupt changes in precipitation patterns.

The trend of decreasing precipitation during the second period was more pronounced than during the first period so that the highest decrease in mean annual precipitation was observed under the RCP8.5 scenario, while precipitation remained almost constant under the RCP2.6 scenario. Z. Li et al. (2019) also reported similar results in the Clear Creek Basin in Texas, USA. According to their results, precipitation decreased more rapidly under the RCP8.5 scenario than the RCP2.6 scenario. Compared with the baseline period, NDVI was increasing at Ramhormoz, Mahshahr, Masjed Soleiman, and Dezful stations under all scenarios while the other stations experienced decreasing NDVI along with diminishing precipitation amounts. This interpretation is supported by Yang et al. (2016), which found a significantly positive relationship between annual precipitation and maximum NDVI, mainly in the outlet of the Shiyang and Shule River. Only 7.64% of the Shule Basin's area (a very dry region) showed a significantly positive relationship between annual precipitation and maximum NDVI, indicating that precipitation may not be the leading regulator of plant growth in this region due to the inconsistency between NDVI, precipitation and temperature.

Table 7. Correlation Coefficients Between NDVI, Temperature, and Precipitation During the Future Periods.

SCENARIO	STATION	INDEX	2016–2045		2046–2075	
			R	T	R	T
RCP2.6	**Ahvaz**	NDVI	−.715*	−.416*	−.797*	−.389*
	Abadan		.594*	−.914*	.797*	−.843*
	Bostan		.977*	−.348	.935*	−.488*
	Dezful		.090	.955*	−.039	.968*
	Izeh		.313	−.954*	.503*	−.970*
	Mahshahr		−.589*	.931*	−.390*	.960*
	Masjedsolyman		.501*	.829*	.290	.826*
	Omidaghjari		.959*	−.558*	.922*	−.431*
	Ramhormoz		.172	.973*	−.018	.977*
RCP4.5	Ahvaz	NDVI	−.689*	−.768*	−.822*	−.337
	Abadan		.326	−.965*	.609*	−.795*
	Bostan		.894*	−.556*	.840*	−.539*
	Dezful		.008	.982*	.157	.977*
	Izeh		.009	−.983*	.488*	−.979*
	Mahshahr		−.606*	.981*	−.555*	.970*
	Masjedsolyman		.273	.938*	.415*	.896*
	Omidaghjari		.883*	−.469*	.902*	−.595*
	Ramhormoz		−.137	.989*	.000	.976*
RCP8.5	Ahvaz	NDVI	−.613*	−.809*	−.730*	−.729*
	Abadan		.452*	−.969*	.156	−.943*
	Bostan		.901*	−.665*	.887*	−.756*
	Dezful		−.351	.980*	−.450*	.991*
	Izeh		.507*	−.990*	.523*	−.993*
	Mahshahr		−.594*	.983*	−.451*	.990*
	Masjedsolyman		−.112	.969*	.173	.968*
	Omidaghjari		.887*	−.559*	.918*	−.790*
	Ramhormoz		−.109	.993*	−.195	.996*

NDVI: normalized difference vegetation index; RCP: representative concentration pathway.
Values in bold are different from 0 with a significance level alpha < .05.
*Significant relationship ($p < .05$).

It can be concluded, based on annual NDVI analysis and its correlation with precipitation and temperature, that the consequences of climate change may not be manifested in the NDVI trends because precipitation affects plants by providing water, while temperature controls the growth of plants under normal conditions, thus NDVI is a product of the complex interactions between climate change and human activities (Burry et al., 2019). Temperature is projected to increase at all stations under the three scenarios and during the two future periods. Moreover, at Ahvaz, Abadan, and Omidieh Aghajari precipitation has increased. In contrast, NDVI is expected to continue to decrease during both future periods. The highest population growth rate, energy use, and, in turn, greenhouse gas emissions are projected to occur under the RCP8.5 scenario, while the RCP2.6 scenario is based on an expectation of the lowest rate of population growth, increased use of renewable energy, and significant reduction of greenhouse gas emissions. The RCP4.5 scenario assumed balanced growth. In projecting the effects of

climate changes on vegetation, the results achieved under the RCP8.5 scenario differed greatly from the other two scenarios because the radiative forcing under this scenario is considered to reach to 8.5 W/m^2 by the end of the 21st century (J. Li et al., 2015). Given that the majority of stations showed increasing temperatures and decreasing precipitation and vegetation, it can be concluded that increasing global population growth and the burgeoning demand for food and energy combined with the limitations posed by climate change have compromised the quantities and qualities of natural resources and will continue to do so in the future. In this research, NDVI data were measured by AVHRR at a resolution of 8 km. For this pixel size, satellite data with lower spatial and temporal resolution are recommended (e.g., Landsat and MODIS, for better examination of vegetation cover). The model, CanESM2, is from the ensemble of the models in the IPCC's fifth report. Data from the sixth report have been made available recently and these can now be analyzed. For better accuracy, it is recommended that several climatic models should be used instead of only a lone model. The best model should be selected by comparisons of their effectiveness to produce the best model.

Conclusion

Global warming has caused significant impacts in terrestrial ecosystems, especially to the vegetation. The long-term impacts of climate change on vegetation dynamics is an important arena of study. This study assessed and simulated the trends of vegetation coverage derived from AVHRR-NDVI data. Moreover, the relationships between observed climate data of weather stations for 1984 to 2015 and CANESM2 model-produced data for two future periods from 2016 to 2045 and 2046 to 2075 under RCP2.6, RCP4.5, and RCP8.5 scenarios were investigated.[AQ14] The first future period is expected to show decreasing vegetation and precipitation and increasing temperatures. A positive relationship was found between NDVI and precipitation, while NDVI is inversely related to temperature. NDVI and precipitation would be expected to decrease during the first period and temperatures might be expected to increase at a statistically significant rate. During the second future period, NDVI and precipitation are expected to decrease, and temperatures are expected to increase. These predictions are statistically significant. It can be concluded that combining RS data with climatic data in large-scale models can generate useful information to inform monitoring and to provide insight to aid in ecosystem planning and policy decisions, and with the management of vegetation and other vital resources.

Author Contributions

H.E.D.: software, formal analysis, investigation, visualization, writing an original draft, and project administration. M.J.: formal analysis, investigation, visualization, and writing original draft. H.E.D.: formal analysis, investigation, visualization, and supervision. M.B.: investigation and visualization. A.K.: investigation, visualization, supervision, writing original draft, review, and editing. J.P.T.: investigation, visualization, writing original draft, review, and editing.

Declaration of Conflicting Interests

The author(s) declared no potential conflicts of interest with respect to the research, authorship, and/or publication of this article.

Funding

The author(s) received no financial support for the research, authorship, and/or publication of this article.

REFERENCES

Afreen, T., & Singh, H. (2019). Does change in precipitation magnitude affect the soil respiration response? A study on constructed invaded and uninvaded tropical grassland ecosystem. *Ecological Indicators*, *102*, 84–94.

Ahmadaali, K., Damaneh, H. E., Ababaei, B., & Damaneh, H. E. (2021). Impacts of droughts on rainfall use efficiency in different climatic zones and land uses in Iran. *Arabian Journal of Geosciences*, *14*(2), 1–15.

Ali, S., Henchiri, M., Yao, F., & Zhang, J. (2019). Analysis of vegetation dynamics, drought in relation with climate over South Asia from 1990 to 2011. *Environmental Science and Pollution Research*, *26*(11), 11470–11481.

Alimoradi, S., Khorani, A., & Esmaeilpour, Y. (2017). Dynamics of vegetation in Karun watershed within Khuzestan province in relation with Temperature factors and precipitation. *Journal of Geographical Sciences*, *17*, 155–177.

Awal, R., Bayabil, H. K., & Fares, A. (2016). Analysis of potential future climate and climate extremes in the Brazos Headwaters basin, Texas. *Water*, 8(12), 603.

Batllori, E., Parisien, M. A., Krawchuk, M. A., & Moritz, M. A. (2013). Climate change-induced shifts in fire for Mediterranean ecosystems. *Global Ecology and Biogeography*, *22*(10), 1118–1129.

Braganza, K., Karoly, D. J., & Arblaster, J. M. (2004). Diurnal temperature range as an index of global climate change during the twentieth century. *Geophysical Research Letters*, *31*(13), L13217.

Burry, L. S., Palacio, P. I., Somoza, M., de Mandri, M. E. T., Lindskoug, H. B., Marconetto, M. B., & D'Antoni, H. L. (2018). Dynamics of fire, precipitation, vegetation and NDVI in dry forest environments in NW Argentina. Contributions to environmental archaeology. *Journal of Archaeological Science: Reports*, *18*, 747–757.

Choi, I. J., Park, R. S., & Lee, J. (2019). Impacts of a newly-developed aerosol climatology on numerical weather prediction using a global atmospheric forecasting model. *Atmospheric Environment*, *197*, 77–91.

Choo, Y. M., Jo, D. J., Yun, G. S., & Lee, E. H. (2019). A study on the improvement of flood forecasting techniques in urban areas by considering rainfall intensity and duration. *Water*, *11*(9), 1883.

Chu, H., Venevsky, S., Wu, C., & Wang, M. (2019). NDVI-based vegetation dynamics and its response to climate changes at Amur-Heilongjiang River Basin from 1982 to 2015. *Science of the Total Environment*, *650*, 2051–2062.

Chuai, X. W., Huang, X. J., Wang, W. J., & Bao, G. (2013). NDVI, temperature and precipitation changes and their relationships with different vegetation types during 1998–2007 in Inner Mongolia, China. *International Journal of Climatology*, *33*(7), 1696–1706.

Cooper, R. T. (2019). Projection of future precipitation extremes across the Bangkok Metropolitan Region. *Heliyon*, *5*(5), Article e01678.

Croke, J., Thompson, C., & Fryirs, K. (2017). Prioritising the placement of riparian vegetation to reduce flood risk and end-of-catchment sediment yields: Important considerations in hydrologically-variable regions. *Journal of Environmental Management*, *190*, 9–19.

D'Oria, M., Ferraresi, M., & Tanda, M. G. (2017). Historical trends and high-resolution future climate projections in northern Tuscany (Italy). *Journal of Hydrology*, *555*, 708–723.

Dore, M. H. (2005). Climate change and changes in global precipitation patterns: What do we know? *Environment International*, *31*(8), 1167–1181.

Duffy, P. B., Brando, P., Asner, G. P., & Field, C. B. (2015). Projections of future meteorological drought and wet periods in the Amazon. *Proceedings of the National Academy of Sciences of the United States of America*, *112*(43), 13172–13177.

El-Samra, R., Bou-Zeid, E., & El-Fadel, M. (2018). What model resolution is required in climatological downscaling over complex terrain? *Atmospheric Research*, *203*, 68–82.

Eskandari, H., Borji, M., Khosravi, H., & Mesbahzadeh, T. (2016). Desertification of forest, range and desert in Tehran province, affected by climate change. *Solid Earth*, *7*(3), 905–915.

Gaitán, E., Monjo, R., Pórtoles, J., & Pino-Otín, M. R. (2019). Projection of temperatures and heat and cold waves for Aragón (Spain) using a two-step statistical downscaling of CMIP5 model outputs. *Science of the Total Environment*, *650*, 2778–2795.

Ghaemi, E., Kavianpour, M., Moazami, S., Hong, Y., & Ayat, H. (2017). Uncertainty analysis of radar rainfall estimates over two different climates in Iran. *International Journal of Remote Sensing*, *38*(18), 5106–5126.

Ghorbani, M., Eskandari-Damaneh, H., Cotton, M., Ghoochani, O. M., & Borji, M. (2021). Harnessing indigenous knowledge for climate change-resilient water management—Lessons from an ethnographic case study in Iran. [published online ahead of print February 4, 2021] *Climate and Development*. doi:10.1080/17565529.2020.1841601

Gorguner, M., Kavvas, M. L., & Ishida, K. (2019). Assessing the impacts of future climate change on the hydroclimatology of the Gediz Basin in Turkey by using dynamically downscaled CMIP5 projections. *Science of the Total Environment*, *648*, 481–499.

Gouveia, C. M., Trigo, R. M., Beguería, S., & Vicente-Serrano, S. M. (2017). Drought impacts on vegetation activity in the Mediterranean region: An assessment using remote sensing data and multi-scale drought indicators. *Global and Planetary Change*, *151*, 15–27.

Hadian, F., Jafari, R., Bashari, H., Tarkesh, M., & Clarke, K. D. (2019). Effects of drought on plant parameters of different rangeland types in Khansar region, Iran. *Arabian Journal of Geosciences*, *12*, 93.

Hansen, J., Sato, M., & Ruedy, R. (2013). Reply to Stone et al.: Human-made role in local temperature extremes. *Proceedings of the National Academy of Sciences of the United States of America*, *110*(17), Article E1544.

Hansen, J., Sato, M., Ruedy, R., Lo, K., Lea, D. W., & Medina-Elizade, M. (2006). Global temperature change. *Proceedings of the National Academy of Sciences of the United States of America*, *103*(39), 14288–14293.

Higginbottom, T. P., & Symeonakis, E. (2014). Assessing land degradation and desertification using vegetation index data: Current frameworks and future directions. *Remote Sensing*, *6*(10), 9552–9575.

Hou, J., Du, L., Liu, K., Hu, Y., & Zhu, Y. (2019). Characteristics of vegetation activity and its responses to climate change in desert/grassland biome transition zones in the last 30 years based on GIMMS3g. *Theoretical and Applied Climatology*, *136*(3), 915–928.

IPCC, 2014: *Climate Change 2014: Synthesis Report. Contribution of Working Groups I, II and III to the Fifth Assessment Report of the Intergovernmental Panel on Climate Change* [Core Writing Team, R.K. Pachauri and L.A. Meyer (eds.)]. IPCC, Geneva, Switzerland, 151 pp

Irving, D. B., Whetton, P., & Moise, A. F. (2012). Climate projections for Australia: A first glance at CMIP5. *Australian Meteorological and Oceanographic Journal*, *62*(4), 211–225.

Ishida, K., Gorguner, M., Ercan, A., Trinh, T., & Kavvas, M. L. (2017). Trend analysis of watershed-scale precipitation over Northern California by means of dynamically-downscaled CMIP5 future climate projections. *Science of the Total Environment*, *592*, 12–24.

Keggenhoff, I., Elizbarashvili, M., Amiri-Farahani, A., & King, L. (2014). Trends in daily temperature and precipitation extremes over Georgia, 1971–2010. *Weather and Climate Extremes*, *4*, 75–85.

Kharuk, V. I., Ranson, K. J., & Dvinskaya, M. L. (2007). Evidence of evergreen conifer invasion into larch dominated forests during recent decades in central Siberia. *Eurasian Journal of Forest Research*, *10*(2), 163–171.

Khosravi, H., Azareh, A., Dameneh, H. E., Sardoii, E. R., & Dameneh, H. E. (2017). Assessing the effects of the climate change on land cover changes in different time periods. *Arabian Journal of Geosciences*, *10*(4), 93.

Lamchin, M., Lee, W. K., Jeon, S. W., Wang, S. W., Lim, C. H., Song, C., & Sung, M. (2018). Long-term trend and correlation between vegetation greenness and climate variables in Asia based on satellite data. *Science of the Total Environment*, *618*, 1089–1095.

Lee, T. M., Markowitz, E. M., Howe, P. D., Ko, C.-Y., & Leiserowitz, A. A. (2015). Predictors of public climate change awareness and risk perception around the world. *Nature Climate Change*, *5*, 1014–1020. https://doi.org/10.1038/nclimate2728

Li, J., Zhang, Q., Chen, Y. D., & Singh, V. P. (2015). Future joint probability behaviors of precipitation extremes across China: Spatiotemporal patterns and implications for flood and drought hazards. *Global and Planetary Change*, *124*, 107–122.

Li, Z., Li, X., Wang, Y., & Quiring, S. M. (2019). Impact of climate change on precipitation patterns in Houston, Texas, USA. *Anthropocene*, *25*, 100193.

Masoudi, M., & Elhaeesahar, M. (2016). Trend assessment of climate changes in Khuzestan Province, Iran. *Natural Environment Change*, *2*(2), 143–152.

Moazami, S., Golian, S., Kavianpour, M. R., & Hong, Y. (2014). Uncertainty analysis of bias from satellite rainfall estimates using copula method. *Atmospheric Research*, *137*, 145–166.

Moriasi, D. N., Arnold, J. G., Van Liew, M. W., Bingner, R. L., Harmel, R. D., & Veith, T. L. (2007). Model evaluation guidelines for systematic quantification of accuracy in watershed simulations. *Transactions of the ASABE*, *50*(3), 885–900.

Muradyan, V., Tepanosyan, G., Asmaryan, S., Saghatelyan, A., & Dell'Acqua, F. (2019). Relationships between NDVI and climatic factors in mountain ecosystems: A case study of Armenia. *Remote Sensing Applications: Society and Environment*, *14*, 158–169.

Ortiz-Jiménez, M. A. (2018). Quantitative evaluation of the risk of *Vibrio parahaemolyticus* through consumption of raw oysters (*Crassostrea corteziensis*) in Tepic, Mexico, under the RCP2.6 and RCP8.5 climate scenarios at different time horizons. *Food Research International*, *111*, 111–119.

Pate, T. M. (2011). Global climate change impacts in the world. *Current World Environment*, *6*(2), 217–223.

Peña-Angulo, D., Nadal-Romero, E., González-Hidalgo, J. C., Albaladejo, J., Andreu, V., Bagarello, V., . . .Zorn, M. (2019). Spatial variability of the relationships of runoff and sediment yield with weather types throughout the Mediterranean basin. *Journal of Hydrology*, *571*, 390–405.

Pereira, H. M., Leadley, P. W., Proença, V., Alkemade, R., Scharlemann, J. P., Fernandez-Manjarrés, J. F., . . .Walpole, M. (2010). Scenarios for global biodiversity in the 21st century. *Science*, *330*(6010), 1496–1501.

Pinzon, J. E., & Tucker, C. J. (2014). A non-stationary 1981–2012 AVHRR NDVI3g time series. *Remote Sensing*, *6*(8), 6929–6960.

Pullens, J. W. M., Sharif, B., Trnka, M., Balek, J., Semenov, M. A., & Olesen, J. E. (2019). Risk factors for European winter oilseed rape production under climate change. *Agricultural and Forest Meteorology*, *272*, 30–39.

Qi, X., Jia, J., Liu, H., & Lin, Z. (2019). Relative importance of climate change and human activities for vegetation changes on China's silk road economic belt over multiple timescales. *Catena*, *180*, 224–237.

Rahimi, J., Ebrahimpour, M., & Khalili, A. (2013). Spatial changes of extended De Martonne climatic zones affected by climate change in Iran. *Theoretical and Applied Climatology*, *112*(3), 409–418.

Rathore, P., Roy, A., & Karnatak, H. (2019). Modelling the vulnerability of *Taxus wallichiana* to climate change scenarios in South East Asia. *Ecological Indicators*, *102*, 199–207.

Rebetez, M. (1996). Public expectation as an element of human perception of climate change. *Climatic Change*, *32*, 495–509. https://doi.org/10.1007/BF00140358

Rodrigo-Comino, J., Senciales, J. M., Sillero-Medina, J. A., Gyasi-Agyei, Y., Ruiz-Sinoga, J. D., & Ries, J. B. (2019). Analysis of weather-type-induced soil erosion in cultivated and poorly managed abandoned sloping vineyards in the Axarquía Region (Málaga, Spain). *Air, Soil and Water Research*, *12*, 1–1. https://doi.org/10.1177/1178622119839403

Savari, M., Eskandari Damaneh, H., & Damaneh, H. E. (2021). Factors influencing farmers' management behaviors toward coping with drought: Evidence from Iran. *Journal of Environmental Planning and Management*. https://doi.org/10.1080/09640568.2020.1855128

Sen, P. K. (1968). Estimates of the regression coefficient based on Kendall's tau. *Journal of the American Statistical Association*, *63*(324), 1379–1389.

Shagega, F. P., Munishi, S. E., & Kongo, V. M. (2019). Prediction of future climate in Ngerengere river catchment, Tanzania. *Physics and Chemistry of the Earth, Parts A/B/C*, *112*, 200–209.

Shimizu, Y., Lu, Y., Aono, M., & Omasa, K. (2019). A novel remote sensing-based method of ozone damage assessment effect on Net Primary Productivity of various vegetation types. *Atmospheric Environment*, *217*, 116947.

Some'e, B. S., Ezani, A., & Tabari, H. (2012). Spatiotemporal trends and change point of precipitation in Iran. *Atmospheric Research*, *113*, 1–12.

Tabari, H., & Talaee, P. H. (2011). Temporal variability of precipitation over Iran: 1966–2005. *Journal of Hydrology*, *396*(3–4), 313–320.

Tošić, I. (2004). Spatial and temporal variability of winter and summer precipitation over Serbia and Montenegro. *Theoretical and Applied Climatology*, *77*, 47–56.

Tucker, C. J., Pinzon, J. E., Brown, M. E., Slayback, D. A., Pak, E. W., Mahoney, R., . . .El Saleous, N. (2005). An extended AVHRR 8-km NDVI dataset compatible with MODIS and SPOT vegetation NDVI data. *International Journal of Remote Sensing*, *26*(20), 4485–4498.

WenBin, Z. H. U., AiFeng, L. V., & ShaoFeng, J. I. A. (2011). Spatial distribution of vegetation and the influencing factors in Qaidam Basin based on NDVI. *Journal of Arid Land*, *3*(2), 85–93.

Wilby, R. L., & Dawson, C. W. (2013). The statistical downscaling model: Insights from one decade of application. *International Journal of Climatology*, *33*(7), 1707–1719.

Wingate, V. R., Phinn, S. R., & Kuhn, N. (2019). Mapping precipitation-corrected NDVI trends across Namibia. *Science of the Total Environment*, *684*, 96–112.

Worku, G., Teferi, E., Bantider, A., Dile, Y. T., & Taye, M. T. (2018). Evaluation of regional climate models performance in simulating rainfall climatology of Jemma sub-basin, Upper Blue Nile Basin, Ethiopia. *Dynamics of Atmospheres and Oceans*, *83*, 53–63.

Wu, J., Xu, Y., & Gao, X. J. (2017). Projected changes in mean and extreme climates over Hindu Kush Himalayan region by 21 CMIP5 models. *Advances in Climate Change Research*, *8*(3), 176–184.

Yan, T., Bai, J., Arsenio, T., Liu, J., & Shen, Z. (2019). Future climate change impacts on streamflow and nitrogen exports based on CMIP5 projection in the Miyun Reservoir Basin, China. *Ecohydrology & Hydrobiology*, *19*(2), 266–278.

Yan, Y., Liu, X., Wen, Y., & Ou, J. (2019). Quantitative analysis of the contributions of climatic and human factors to grassland productivity in northern China. *Ecological Indicators*, *103*, 542–553.

Yang, X., Liu, S., Yang, T., Xu, X., Kang, C., Tang, J., . . .Li, Z. (2016). Spatial-temporal dynamics of desert vegetation and its responses to climatic variations over the last three decades: A case study of Hexi region in Northwest China. *Journal of Arid Land*, *8*(4), 556–568.

Zhang, D. F., Han, Z. Y., & Shi, Y. (2017). Comparison of climate projections between driving CSIRO-Mk3. 6.0 and downscaling simulation of RegCM4. 4 over China. *Advances in Climate Change Research*, *8*(4), 245–255.

Zhang, H. K., & Roy, D. P. (2016). Landsat 5 Thematic Mapper reflectance and NDVI 27-year time series inconsistencies due to satellite orbit change. *Remote Sensing of Environment*, *186*, 217–233.

Zhang, Y., Gao, J., Liu, L., Wang, Z., Ding, M., & Yang, X. (2013). NDVI-based vegetation changes and their responses to climate change from 1982 to 2011: A case study in the Koshi River Basin in the middle Himalayas. *Global and Planetary Change*, *108*, 139–148.

Zhao, A., Zhang, A., Cao, S., Liu, X., Liu, J., & Cheng, D. (2018). Responses of vegetation productivity to multi-scale drought in Loess Plateau, China. *Catena*, *163*, 165–171.

Zheng, Y., Han, J., Huang, Y., Fassnacht, S. R., Xie, S., Lv, E., & Chen, M. (2018). Vegetation response to climate conditions based on NDVI simulations using stepwise cluster analysis for the Three-River Headwaters region of China. *Ecological Indicators*, *92*, 18–29.